

# A deep generative model for single-cell RNA sequencing with application to detecting differentially expressed genes

Romain Lopez<sup>†</sup>, Jeffrey Regier<sup>†</sup>, Michael Cole<sup>††</sup>, Michael Jordan<sup>†</sup> and Nir Yosef<sup>†</sup>

<sup>†</sup> Department of Electrical Engineering and Computer Sciences, University of California, Berkeley

<sup>††</sup> Department of Physics, University of California, Berkeley

{romain\_lopez, regier, mbcole, jordan, niryosef}@berkeley.edu

Single-cell RNA sequencing (scRNA-Seq) is a revolutionary technology, which allows studying fundamental biological questions that were previously out of reach [1, 2]. It allows, for the first time, to reveal a cell’s identity and characterize its molecular circuitry in an unbiased, data-driven way. The product of a scRNA-Seq experiment is a data matrix  $X$  where entry  $X_{ng}$  approximates the number of transcripts of gene  $g$  in cell  $n$ . Careful computational analysis allows deriving from such data exciting insights in diverse biomedical fields [3, 4]. While it is typical to observe thousands of gene products per cell, many transcripts are observed very infrequently, and for technical reasons related to the method of sequencing these are particularly prone to high variance. Additionally, due to the limited transcript capture efficiency inherent to RNA-Seq protocols, entries of  $X$  are typically zero-inflated [5].

While there is often little prior knowledge of single-cell heterogeneity generating  $X$ , a reasonably general assumption is that  $X$  has been generated from a low-dimensional manifold of cellular states [1]. Therefore, numerous dimensionality reduction techniques have been proposed for interpreting  $X$  (e.g., to facilitate clustering, visualization, and data imputation). Each technique has shortcomings, however. Most are based on linear models of the data [5, 6, 7] though there is no basis for assuming linearity. Most are optimized with batch algorithms, preventing them from scaling beyond thousands of cells [5, 6, 8]. However, sequencing millions of cells is becoming possible [9]. The best performing method to date [6] is particularly complicated to train, involving numerous subroutines for alternating minimization. Recent articles apply neural networks, but without an architecture based on biology [10, 11].

We propose Single-cell Variational Inference (scVI), a probabilistic inference procedure based on a fully generative model. In scVI, some conditional distributions are specified by neural networks that encode complex, nonlinear relationships, learned from large datasets. scVI explicitly models technical effects, so as to “disentangle” them from a low-dimensional vector that represents the cells’ underlying states.

After describe our generative model (Section 1) and an inference procedure for it (Section 2), we compare scVI to alternative methods on three benchmarks tasks (Section 3). Finally, we introduce a Bayesian hypothesis testing procedure that leverages scVI to find differentially expressed genes (Section 4). Our source code, based on TensorFlow, is publicly available at <https://github.com/YosefLab/scVI>.

## 1 The scVI probabilistic model

Figure 1 represents the probabilistic model graphically. Latent variable

$$z_n \sim \mathcal{N}(0, I)$$

is a low-dimensional random vector describing cell  $n$ . For neural network  $f_w$ , latent variable

$$w_{ng} \sim \text{Gamma}(f_w(z_n, \gamma_n))$$

accounts for the stochasticity of gene  $g$  expressed in cell  $n$ . Here the constant  $\gamma_n$  are optional covariates that can be passed to  $f_w$  that account for batch effects, like normalization [12, 13], to remove unwanted variation from the latent representation. Latent variable

$$y_{ng} \sim \text{Poisson}(w_{ng})$$

is the underlying expression level for gene  $g$  in cell  $n$ .

For neural network  $f_h$ , latent variable

$$h_{ng} \sim \text{Bernoulli}(f_h(z_n, \gamma_n))$$

indicates whether a particular entry has been “zeroed out” due to technical effects [5, 6].

Finally, the observed gene expression level is defined by:

$$x_{ng} = \begin{cases} y_{ng} & \text{if } h_{ng} = 0, \\ 0 & \text{otherwise.} \end{cases}$$

Conditional distribution  $p(x_{ng}|z_n)$  is a zero-inflated negative binomial—a distribution known to effectively model the kinetics of stochastic gene expression with some entries replaced by zeros [14].

The neural networks  $f_w$  and  $f_h$  use dropout regularization and batch normalization. Each network has 3 fully connected-layers, with 128 nodes each. The activation functions are all ReLU, exponential, or linear. Weights for some layers are shared between  $f_w$  and  $f_h$ .

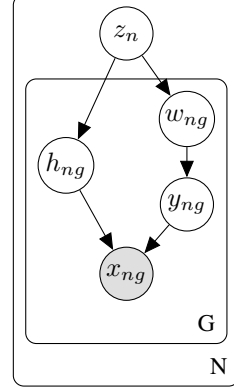


Figure 1: The scVI graphical model

## 2 Posterior inference

The posterior distribution combines the prior knowledge with information acquired from the data  $X$ . We cannot directly apply Bayes rule to determine the posterior because the denominator (the marginal distribution)  $p(x_n)$  is intractable.

Instead, we use variational inference [15] to approximate the posterior  $p(x_n|z_n)$ . Our variational distribution  $q(z_n|x_n)$  is Gaussian with a diagonal covariance matrix. The variational distribution’s mean and covariance are given by an encoder network applied to  $x_n$ , as in [16]. The encoder network may, optionally, be given the constant covariates  $\gamma_n$  (along with  $x_n$ ) if we wish to discourage  $z_n$  from encoding batch effects and other unwanted variations.

The variational lower bound is

$$\mathcal{L}(n) \geq \mathbb{E}_{q(z|x)} \log p(x|z) - KL(q(z|x)||p(z)) \quad (1)$$

To optimize the variational lower bound, we write  $p(x|z)$  by analytically marginalizing out the discrete random variables  $h_{ng}$ ,  $w_{ng}$ , and  $y_{ng}$ . Now, our variational lower bound is continuous and end-to-end differentiable. We maximize the variational lower bound using stochastic backpropagation.

## 3 Performance benchmarks

We assess the performance of scVI at three benchmark tasks: generalizing to heldout data (Section 3.1), imputating “zeroed out” data (Section 3.2), and recovering known clusters (Section 3.3). Throughout, we compare scVI with factor analysis, as well as two state-of-the-art methods: ZIFA [5] and ZINB-WaVE [6]

Only scVI and factor analysis scale to the larger benchmark datasets—a key advantage relative to ZIFA and ZINB-WaVE. ZIFA and ZINB-WaVE are based on batch optimization algorithms. Their runtimes for *each* iteration of their numerical optimization routines scale linearly in the number of samples and linearly in the number of genes—both potentially very large. For 10,000 cells, each of these methods requires more than 20 minutes of computation. For 100,000 cells, both methods run out of memory on a machine with 32 GB RAM. scVI trains on the entire 1.3 million cell dataset in less than two hours on a single GPU, using off-the-shelf neural network software.

### 3.1 Generalization to heldout data

For this task, we use a dataset that contains 1.3 million brain cells from 10x GENOMICS [9] with 720 sampled variable genes. For each method, we learn a mapping from the 10-dimensional latent space to a reconstruction of training set  $X$ . Then, we assess the marginal likelihood of held-out data, conditioned on a latent representation learned for the held-out data by each model. Table 1 shows that scVI best compresses the held-out data, even for our smallest dataset. scVI’s lead over the other methods grows as the dataset size grows.

cells	4k	10k	100k
FA	-1178.2	-1177.3	-1169.8
ZIFA	-1250.9	-1250.7	NA
ZINB-WaVE	-1166.3	-1164.4	NA
scVI	<b>-1159.9</b>	<b>-1147.8</b>	<b>-1128.73</b>

Table 1: Marginal log likelihood for a held-out subset of the brain cells dataset. NA means we could not run the given algorithm for this sample size.

	imputation error	identification of zeroed-out
ZIFA	3.00	1.955
MAGIC	1.806	NA
ZINB-WaVE	1.053	1.366
scVI	<b>1.048</b>	<b>0.742</b>

Table 2: Absolute errors for imputing zeroed entries (column 1), mean cross entropy for predicting which entries were zeroed-out entries (column 2). Scores are based on a dataset of 10,000 brain cells. MAGIC does not predict dropout probabilities.

### 3.2 Imputating zeroed-out data

On a 10,000 sample of the same dataset, we set to zero entries at random conditioned on the expected transcript abundance — according to probabilities from the ZIFA model — to mimic the technical effects that zero out some entries of the real data. Because we have introduced these zeros synthetically, we know 1) each entry’s true value, and 2) that each entry is zero because of a technical effect, not because the true expression level is nearly zero. We also compare for this task to a state-of-the-art method MAGIC [17] based on diffusion in the cell k-nearest neighbors graph and report results on Table 2.

### 3.3 Recovering known clusters

To further assess the models, we compare how each clusters cells of known types (e.g., muscle cells, blood cells) in latent space. For this task, we make a slight modification to our model: we treat each  $z_n$  as an unknown parameter to estimate rather than a latent variable with a distribution. This way, our procedure maximizes mutual information between  $z_n$  and  $x_n$  [18].

A first dataset from [19] contains 3005 mouse cortex cells and gold-standard labels for seven distinct cell types. Each cell type corresponds to a cluster to recover. We sample 558 variable genes as in [8] and report silhouette (a measure of distance between clusters) on the mouse cortex dataset in Table 3.

A second dataset contains 12039 Peripheral blood mononuclear cells (PBMCs) from [20] with 10310 sampled genes and get biologically meaningful clusters with the software Seurat [21]. For this dataset, we use SCONE [22] to select most important factors of unwanted variation to be incorporated into downstream models. These factors generally include batches meta-data, sequencing depth (number of transcript per cell) and quality controls (QC) for each cell. In this case, SCONE selected a strategy that consists in scaling by depth and regressing out the QC.

	silhouette
FA	0.208
ZIFA	0.202
ZINB-WaVE	0.260
scVI	<b>0.285</b>

Table 3: Silhouette scores on the mouse cortex dataset.

	silhouette (higher is better)	QC correlation (lower is better)
PCA	0.314	0.381
PCA (normalized)	0.321	0.169
scVI (no covariates)	0.375	0.366
scVI	<b>0.379</b>	<b>0.157</b>

Table 4: Unwanted variation metric on the PBMCs dataset.

We compare scVI with and without covariates with a PCA with and without normalization in Table 4 and show we can better remove the variation while yielding a high silhouette score — which means we would get a consistent but tighter clustering with our latent space.

## 4 Differential expression

A significant application of our generative model and of main interest in the field is to go from a clustering to a procedure for identifying gene differentially expressed between two cell-types. Our model relies on Bayesian statistics and can thus benefit from uncertainty evaluation to provide a hypothesis testing framework for differential expression.

Let  $A$  and  $B$  be two set of cells and  $g$  a fixed gene. Now take  $(a, b) \in A \times B$  and say we want to test the following:

$$\mathcal{H}_0^g : w_{ag} < w_{bg} \quad \text{vs.} \quad \mathcal{H}_1^g : w_{ag} \geq w_{bg}$$

where  $w$  is the Gamma latent variable in the generative model, i.e the mean of the gene expression conditioned on a non-dropout event. The posterior of these hypotheses can be approximated via the variational distribution:

$$p(\mathcal{H}_0^g | x) \approx \iint_{z_a, z_b, w_{ag}, w_{bg}} p(w_{ag} < w_{bg}) dp(w_{ag} | z_a) dq(z_a | x_a) dp(w_{bg} | z_b) dq(z_b | x_b)$$

where all the measures are uni-dimensional or low-dimensional so we can use naive monte-carlo to compute these integrals. We can then use a Bayes factor for the test.

We use again the PBMC dataset from [20] and the Seurat-based cell classification to understand how differential expression is captured by our testing method compared to tradition DESeq2 [23]. We defined a reference from a publicly-available bulk array expression profiling data for human B cells (n=10) and Dendritic cells (n=10) at baseline of vaccination [24] which we use to test the association of each gene's expression with biological class, defining a 2-sided t-test p-value per gene.

Because defining a threshold and then use a ROC curve is ambiguous we prefer to look at reproducibility between the microarray experiment and a family of tests used on the scRNA-Seq sequencing experiment. To quantify this, we model the relationship between significance ranks using the Irreproducible Discovery Rate model for matched rank lists [25] and report correlation score of the reproducible components in Figure 2.

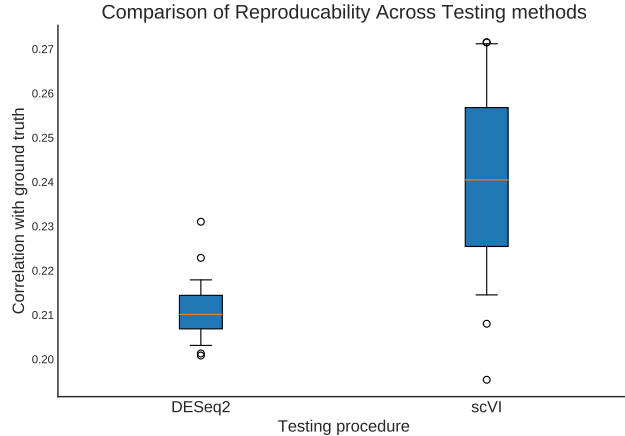


Figure 2: Results on the Differential expression task on B cells against DC cells

## References

- [1] Allon Wagner, Aviv Regev, and Nir Yosef. Revealing the vectors of cellular identity with single-cell genomics. *Nature Biotechnology*, 34(11):1145–1160, 2016.
- [2] Amos Tanay and Aviv Regev. Scaling single-cell genomics from phenomenology to mechanism. *Nature*, 541(7637):331–338, 2017.
- [3] Hongkui Zeng and Joshua R Sanes. Neuronal cell-type classification: challenges, opportunities and the path forward. *Nature Reviews Neuroscience*, 18, 2017.
- [4] Michael J T Stubbington, Orit Rozenblatt-Rosen, Aviv Regev, and Sarah A Teichmann. Single-cell transcriptomics to explore the immune system in health and disease. *Science*, 358(6359):58–63, oct 2017.
- [5] Emma Pierson and Christopher Yau. ZIFA: Dimensionality reduction for zero-inflated single-cell gene expression analysis. *Genome Biology*, 16(1):241, 2015.
- [6] Davide Risso, Fanny Perraudeau, Svetlana Gribkova, Sandrine Dudoit, and JP Vert. ZINB-WaVE: A general and flexible method for signal extraction from single-cell RNA-seq data. *bioRxiv*, 2017.
- [7] David Detomaso and Nir Yosef. FastProject: A tool for low-dimensional analysis of single-cell RNA-Seq data. *DeTomaso BMC Bioinformatics*, 17, 2016.
- [8] Sandhya Prabhakaran, Elham Azizi, and Dana Pe’er. Dirichlet process mixture model for correcting technical variation in single-cell gene expression data. *Proceedings of The 33rd International Conference on Machine Learning*, 48:1070–1079, 2016.
- [9] 10x genomics, 1.3 million brain cells from e18 mice, 2017.
- [10] Jiarui Ding, Anne E. Condon, and Sohrab P Shah. Interpretable dimensionality reduction of single cell transcriptome data with deep generative models. *bioRxiv*, 2017.
- [11] Chieh Lin, Siddhartha Jain, Hannah Kim, and Ziv Bar-Joseph. Using neural networks for reducing the dimensions of single-cell RNA-Seq data. *Nucleic Acids Research*, 2017.
- [12] Catalina A Vallejos, Davide Risso, Antonio Scialdone, Sandrine Dudoit, and John C Marionni. Normalizing single-cell RNA sequencing data: challenges and opportunities. *Nature Methods*, 14(6):565–571, 2017.
- [13] Davide Risso, John Ngai, Terence P Speed, and Sandrine Dudoit. Normalization of RNA-seq data using factor analysis of control genes or samples. *Nature Biotechnology*, 32(9):896–902, 2014.
- [14] Dominic Grun, Lennart Kester, and Alexander van Oudenaarden. Validation of noise models for single-cell transcriptomics. *Nature Methods*, 11(6):637–640, 2014.
- [15] David M Blei, Alp Kucukelbir, and Jon D McAuliffe. Variational inference: A review for statisticians. *Journal of the American Statistical Association*, 2017.
- [16] Diederik P Kingma and Max Welling. Auto-Encoding Variational Bayes. *The International Conference on Learning Representations*, 2014.
- [17] David van Dijk, Juozas Nainys, et al. MAGIC: A diffusion-based imputation method reveals gene-gene interactions in single-cell RNA-sequencing data. *bioRxiv*, page 111591, 2017.
- [18] Shengjia Zhao, Jiaming Song, and Stefano Ermon. Infovae: Information maximizing variational autoencoders. *arXiv preprint arXiv:1706.02262*, 2017.
- [19] Amit Zeisel, Ana B. Muñoz-Manchado, Simone Codeluppi, Peter Lönnerberg, Gioele La Manno, Anna Juréus, Sueli Marques, Hermany Munguba, Liqun He, Christer Betsholtz, Charlotte Rolny, Gonçalo Castelo-Branco, Jens Hjerling-Leffler, and Sten Linnarsson. Cell types in the mouse cortex and hippocampus revealed by single-cell rna-seq. *Science*, 347(6226):1138–1142, 2015.
- [20] Grace X Y Zheng, Jessica M Terry, Phillip Belgrader, Paul Ryvkin, Zachary W Bent, Ryan Wilson, Solongo B Ziraldo, Tobias D Wheeler, Geoff P. McDermott, Junjie Zhu, Mark T Gregory, Joe Shuga, Luz Montesclaros, Jason G Underwood, Donald A Masquelier, Stefanie Y Nishimura, Michael Schnall-Levin, Paul W Wyatt, Christopher M. Hindson, Rajiv Bharadwaj, Alexander Wong, Kevin D Ness, Lan W Beppu, H Joachim Deeg, Christopher McFarland, Keith R Loeb, William J Valente, Nolan G Ericson, Emily A Stevens, Jerald P Radich, Tarjei S Mikkelsen, Benjamin J Hindson, and Jason H Bielas. Massively parallel digital transcriptional profiling of single cells. *Nature Communications*, 8:14049, 2017.

- [21] Evan Macosko, Anindita Basu, Rahul Satija, James Nemesh, Karthik Shekhar, Melissa Goldman, Itay Tirosh, Allison Bialas, Nolan Kamitaki, Emily Martersteck, John Trombetta, David Weitz, Joshua Sanes, Alex Shalek, Aviv Regev, and Steven McCarroll. Highly parallel genome-wide expression profiling of individual cells using nanoliter droplets. *Cell*, 161(5):1202–1214, 2017.
- [22] M. Cole and D. Risso. Single cell overview of normalized expression data, r package version 0.99.6, 2016.
- [23] Michael I. Love, Wolfgang Huber, and Simon Anders. Moderated estimation of fold change and dispersion for rna-seq data with deseq2. *Genome Biol*, 15(12):550, 2014.
- [24] Bulk array profiling data used as biological ground truth, 2011.
- [25] Qunhua Li, James B Brown, Haiyan Huang, and Peter J Bickel. Measuring reproducibility of high-throughput experiments. *Annals of Applied Statistics*, 5(3):1752–1779, 2011.